RESEARCH PAPERS

Acta Cryst. (1996). B52, 899–904

Villamaninite, a Case of Noncubic Pyrite-Type Structure

C. MARCOS,[a] A. PANIAGUA,[a] D. B. MOREIRAS,[a] S. GARCÍA-GRANDA[b]* AND M. R. DIAZ[b]

[a]*Departamento de Geologia, Universidad de Oviedo, Arias de Velasco s/n, 33005 Oviedo, Spain, and* [b]*Departamento de Química Física y Analítica, Universidad de Oviedo, Julián Clavería s/n, 33006 Oviedo, Spain. E-mail: sgg@dwarf1.quimica.uniovi.es*

(*Received 10 December 1992; accepted 29 February 1996*)

Abstract

This paper reports the results obtained in a study of the crystal structure of two villamaninite samples from Villamanín (León, Spain), labeled (1) and (2). Villamaninite, $(Cu,Ni,Co,Fe)(S,Se)_2$, is a pyrite-type disulfide. Different long-period elements, including Au, in ionic substitution are also observed. Previous authors have assumed a cubic $Pa\bar{3}$ symmetry for this mineral. The result of our single crystal study shows a deviation from the cubic symmetry $Pa\bar{3}$ pyrite-type to a pseudocubic symmetry, which is in agreement with the observed optical anisotropy shown by both samples. The structural refinement process leads to a monoclinic model, space group $P12_11$, with $a = 5.709(2)$, $b = 5.707(2)$, $c = 5.708(2)$ Å, $\beta = 90.01(1)°$ for sample (1), and $a = 5.704(3)$, $b = 5.703(3)$, $c = 5.704(3)$ Å, $\beta = 89.99(2)°$ for sample (2), with $Z = 4$. Previous Mössbauer spectroscopic studies stating two different cation sites for Au support the monoclinic model.

1. Introduction

Disulfides of the transition elements show affinity to crystallize in the pyrite-type structure. The Fe, Co, Ni and Cu members of this group occur as minerals – pyrite, cattierite, vaesite and villamaninite – respectively showing different ranges of solid solution among them.

A number of minerals with the pyrite-type crystal structure (cobalite, Giese & Kerr, 1965; pyrite, Gibbons, 1967; Bayliss, 1977*b*; Stanton, 1975; gersdorffite, Bayliss & Stephenson, 1968; willyamite, Cabri, Harris, Stewart & Roland, 1970; arsenian ullmannite, Bayliss, 1977*a*; synthetic CuS_2, King & Prewitt, 1979) have been recognized as pseudocubic. Some of these authors disagree as to whether the optical anisotropy observed in most samples examined is entirely a surface feature or intrinsic to the crystal structure (Bayliss, 1989). There is also disagreement with respect to the X-ray diffraction studies on FeS_2. Finklea, Cathey & Amma (1976) found no deviations from cubic symmetry, but Bayliss (1977*b*) concludes that at least some pyrite crystals are in fact triclinic.

The optical anisotropy observed for CuS_2 (Taylor & Kullerud, 1972) and FeS_2 has raised questions about the correct symmetry of these structures. King & Prewitt (1979) conclude no structural evidence has been found for symmetry lower than cubic in CuS_2, in spite of the optical anisotropy observed in polished sections of this compound. A similar degree of anisotropy in FeS_2 may indicate that some of these crystals are not cubic. However, these authors believe the refinement by Bayliss on the FeS_2 does not adequately test this possibility.

Villamaninite, $(Cu,Ni,Co,Fe)(S,Se)_2$, is a pyrite-type disulfide (Schoeller & Powell, 1920), assumed after recent detailed electron-probe microanalyses on samples of the type locality (Paniagua, 1989) and a new discovery in a hydrothermal chimney from the South Pacific (Oudin, Marchig, Risch, Lalou & Brichet, 1990) to include the end-member CuS_2. After a previous X-ray study (Bayliss, 1977*c*; Ypma, Evers & Woensdregt, 1968; Ramdohr, 1980) cubic ($Pa\bar{3}$) symmetry has been assumed for this mineral. However, reflected-light microscopic studies reveal weakly anisotropic effects (Ypma *et al.*, 1968; Ramdohr, 1980; Paniagua, 1989; Oudin *et al.*, 1990), suggesting a symmetry lower than cubic. These anisotropic effects increase with the Cu content. Also, Cu-rich members usually show up to more than 1 wt % of trace elements in ionic substitution. Zn is the most common, but a high number of long-period elements – including precious metals – is observed. From electron probe microanalysis (Paniagua, 1991) and Mössbauer spectroscopy (Friedl, Paniagua & Wagner, 1991) the possibility of different cation sites and direct as well as coupled substitution are suggested. Both types of substitution have also been observed for Au-bearing arsenopyrite (Johan, Marcoux & Bonnemaison, 1989; Marcoux, Bonnemaison, Braux & Johan, 1989), a monoclinic derivative of pyrite-type structure. Also, calaverite

Table 1. *R_{int} values in different Laue classes, corresponding to the primitive subgroups of space group $Pa\bar{3}$*

	Laue class	R_{int} (1)	R_{int} (2)
Cubic	$m\bar{3}$	0.143	0.088
	$m\bar{3}m$	0.266	0.197
Tetragonal	$4/mmm$	0.223	0.194
	$4/m$	0.212	0.193
Orthorhombic	mmm	0.060	0.060
Monoclinic	$2/m$	0.060	0.054

$R_{int} = \sum(I - \langle I \rangle)/\sum I$.

($AuTe_2$, monoclinic) is another pyrite-type structure with different cation sites (Pertlik, 1984). For these reasons we decided to investigate the villamaninite crystal structure to provide further information on this intriguing problem.

2. Experimental

Two selected crystals of villamaninite were carefully extracted from two polished sections – labeled (1) and (2) – of samples of the type-locality (Providencia mine, Cármenes near Villamanín, Spain). The crystals were opaque, greyish purple and dark, with reflectance ranging between sphalerite and magnetite mean values (Paniagua, Marcos, Moreiras & González, 1987) and weakly anisotropic in orange–red to greenish blue colors under reflected-light microscopy. Sample (1) is darker, showing more intensive purplish hue and optical anisotropy.

The data collection was performed using an Enraf–Nonius CAD-4 single crystal diffractometer with graphite-monochromatized Mo$K\alpha$ radiation, $\lambda = 0.71073$ Å. The crystals were mounted in a random orientation.

A first attempt of the structure refinement on the basis of the $Pa\bar{3}$ space group failed, leading to very high R factors, including the attempts of refining disordered structural models. Systematic attempts on all primitive subgroups of the $Pa\bar{3}$ space group failed because of high R factors, >0.25, or the presence of forbidden reflections in some of the considered groups, except for the lower symmetries. Therefore, a new attempt at structure determination was made with space groups of lower symmetry and the first satisfactory results were obtained in space group $P2_12_12_1$ for samples (1) and (2), leading to R and wR factors lower than 0.06, but inconsistent anisotropic temperature factors (Moreiras, Marcos, Díaz-Fernández & García-Granda, 1991). At this point the reflections measured were for orthorhombic symmetry as a maximum.

The ambiguity in establishing the spacing group of villamaninite led us to carry out a further systematic study, after measuring more reflections. First, the R_{int} values were obtained for the space groups corresponding to the cubic, tetragonal, orthorhombic and monoclinic Laue classes. For the monoclinic class each axis has been treated as unique. Table 1 collects the R_{int} values and it can be observed that the best results are for monoclinic and orthorhombic groups.

On the basis of R_{int} values and the previous attempts of structure determination with primitive subgroups of the $Pa\bar{3}$ space group, we decided to refine the structure of the villamaninite in space group $P12_11$.

This space group was confirmed from structural determination, since the pseudocubic symmetry also includes the systematic absences. Profile analyses were performed on all reflections (Lehmann & Larsen, 1974; Grant & Gabe, 1978).

The starting model included isotropic temperature factors, but no correction for secondary extinction. Subsequent models included anisotropic thermal parameters. The temperature factors of two of the anions of sample (1) are isotropic, being anisotropic for the remaining anions and cations of both samples.

Further refinement in $P12_11$ for metal ordering in the two cation sites for samples (1) and (2) provides R and wR factors higher than those obtained when the metals were disordered, although differences are small.

The different experimental conditions and results from structure refinements in $P12_11$, for both samples, are summarized in Table 2.* Computer programs used: *DATAR* (local programs), *SHELX*76 (Sheldrick, 1976), *SHELXS*86 (Sheldrick, 1985), *PLUTO* (Motherwell & Clegg, 1978) and *PARST* (Nardelli, 1983).

3. Results and discussion

Positional and thermal parameters in $P12_11$ are shown in Table 3 for samples (1) and (2), respectively. Fig. 1 shows the projection of the metals (M) and nonmetals (S) of sample (1) on the (010) plane; the projection of sample (2) atoms is similar. The two types of coordination polyhedra are also shown in Fig. 1.

Octahedral sites are often distorted from $m\bar{3}m$ symmetry by two limiting types of distortion (Robinson, Gibbs & Ribbe, 1971): trigonal distortion of the octahedron along a $\bar{3}$ axis and quadratic distortion along a 4 axis. For pyrite-type structures the amount of octahedral distortion is considered a function of size of the metal atoms, according to King & Prewitt (1979). Quadratic elongation values determined by these authors, for the first-row transition-element pyrites, show that FeS_2 has the most distorted octahedron and that the distortion decreases through CuS_2. The values obtained for villamaninite are 1.0048 and 1.0038 for

* Lists of anisotropic displacement parameters and structure factors have been deposited with the IUCr (Reference: HU1045). Copies may be obtained through The Managing Editor, International Union of Crystallography, 5 Abbey Square, Chester CH1 2HU, England.

Table 2. *Experimental details*

	(1)	(2)
Crystal data		
Chemical formula	$(Cu_{0.68}Ni_{0.15}Co_{0.06}Fe_{0.11})S_{1.97}Se_{0.03}$	$(Cu_{0.53}Ni_{0.27}Co_{0.13}Fe_{0.07})S_{1.98}Se_{0.02}$
Chemical formula weight	127.224	126.160
Cell setting	Monoclinic	Monoclinic
Space group	$P2_1$	$P2_1$
a (Å)	5.709 (2)	5.704 (3)
b (Å)	5.707 (2)	5.703 (3)
c (Å)	5.708 (2)	5.704 (3)
β (°)	90.01 (1)	89.99 (2)
V (Å^3)	186.0 (1)	185.5 (2)
Z	4	4
D_x (Mg m^{-3})	4.54	4.52
Radiation type	Mo $K\alpha$	Mo $K\alpha$
Wavelength (Å)	0.71073	0.71073
No. of reflections for cell parameters	25	25
θ range (°)	26–29	26–29
μ (mm^{-1})	13.200	12.858
Temperature (K)	293	293
Crystal form	Regular	Regular
Crystal size (mm)	0.10 × 0.10 × 0.10	0.10 × 0.10 × 0.10
Crystal color	Greyish purple	Greyish purple
Data collection		
Diffractometer	Enraf–Nonius CAD-4	Enraf–Nonius CAD-4
Data collection method	ω–2θ	ω–2θ
Absorption correction	None	None
No. of measured reflections	4290	4705
No. of independent reflections	1611	1611
No. of observed reflections	539	637
Criterion for observed reflections	$I > 3\sigma(I)$	$I > 3\sigma(I)$
R_{int}	0.060	0.054
θ_{max} (°)	45	45
Range of h, k, l	$-11 \rightarrow h \rightarrow 11$ $-11 \rightarrow k \rightarrow 11$ $-11 \rightarrow l \rightarrow 11$	$-11 \rightarrow h \rightarrow 11$ $-11 \rightarrow k \rightarrow 11$ $-11 \rightarrow l \rightarrow 4$
No. of standard reflections	3	3
Frequency of standard reflections	60	60
Intensity decay (%)	0.94–1.02	0.99–1.09
Refinement		
Refinement on	F	F
R	0.051	0.034
wR	0.051	0.033
S	0.6521	0.9515
No. of reflections used in refinement	539	637
No. of parameters used	51	61
Weighting scheme	$w = 1/[\sigma^2(F_o) + 0.01F_o^2]$	$w = 1/[\sigma^2(F_o) + 0.001F_o^2]$
$(\Delta/\sigma)_{max}$	0.3	0.4
$\Delta\rho_{max}$ (e Å^{-3})	3.67	1.40
$\Delta\rho_{min}$ (e Å^{-3})	−2.93	−1.17
Extinction method	None	None
Source of atomic scattering factors	*International Tables for X-ray Crystallography* (1974, Vol. IV)	*International Tables for X-ray Crystallography* (1974, Vol. IV)

both polyhedra ($M1$ and $M2$) for sample (1) and 1.0044 and 1.0041 for $M1$ and $M2$ polyhedra for sample (2). The distorted octahedra show two sets of values for the edges, those close to 3.5 Å and those close to 3.3 Å, and the $\bar{3}$ axis is destroyed by slight differences in the edge lengths, so that all formal symmetry is lost. The metal sites are also off-center in these polyhedra. The volumes for the $M1$ and $M2$ polyhedra are 18.61 and 18.59 Å^3 for sample (1) and 18.44 and 18.54 Å^3 for sample (2). The volume difference between the two $M1$ and $M2$ polyhedra is so small that it is not possible to show cationic preference in any of them. The result of the refinement for metal ordering does not show cationic preference for any of the two crystallographic sites.

The quadratic elongation values determined for the four tetrahedra of sample (1) are 1.0165, 1.0164, 1.0222 and 1.0232 and the volume values are 6.22, 6.25, 6.36 and 6.31 Å^3, respectively. For sample (2) the quadratic elongation values are 1.0181, 1.0226, 1.0191 and 1.0153 and the volume values are 6.25, 6.28, 6.34 and 6.32 Å^3, respectively. As in the $M1$ and $M2$ octahedra, the tetrahedra lose all their symmetry.

The atomic coordinates of pyrite (Wyckoff, 1963) as well as the transformed coordinates of the monoclinic villamaninite and the differences (Δ) among them are collected in Table 4, taking into account that the coordinate transformation from the monoclinic cell of villamaninite to the cubic cell of pyrite is by

Table 3. *Fractional atomic coordinates and equivalent isotropic displacement parameters (Å²)*

$U_{eq} = (1/3)\Sigma_i\Sigma_j U_{ij} a_i^* a_j^* \mathbf{a}_i.\mathbf{a}_j$.

	x	y	z	U_{eq}
(1)				
$M(1)$	0.7591 (9)	0.100	0.494 (1)	0.0078 (5)
$M(2)$	1.2513 (9)	0.107 (2)	−0.002 (1)	0.0090 (4)
S(1)	0.855 (1)	0.004 (2)	0.101 (2)	0.013 (2)
S(2)	1.150 (2)	0.003 (3)	0.602 (2)	0.013 (2)
S(3)	0.647 (1)	0.212 (2)	0.894 (1)	0.006 (2)
S(4)	0.357 (1)	0.211 (3)	0.395 (1)	0.008 (2)
(2)				
$M(1)$	0.7475 (8)	0.100	0.4975 (9)	0.0095 (2)
$M(2)$	1.2483 (7)	0.103 (1)	0.0019 (9)	0.0093 (2)
S(1)	0.853 (1)	−0.002 (1)	0.106 (1)	0.011 (1)
S(2)	1.137 (1)	−0.007 (2)	0.606 (1)	0.010 (1)
S(3)	0.644 (1)	0.208 (1)	0.896 (1)	0.007 (1)
S(4)	0.3471 (9)	0.204 (1)	0.397 (1)	0.0059 (8)

$-x, \frac{1}{2}-z, y+\frac{1}{2}$ and the displacements on the y and x axes. The differences between the pyrite and the monoclinic villamaninite coordinates are lower than 0.01 for the metals and 0.02 for the nonmetals.

The metal and nonmetal ordering causes all of the threefold axes, the glide planes and the twofold axes, except that parallel to the y axis, of the $Pa\bar{3}$ space group to disappear.

Interatomic distances and angles of the first coordination polyhedra calculated from the final model for M (metal) and S (nonmetal) in the two studied samples in the $P12_11$ space group are listed in Table 5. The bond lengths S—S and bond angles $M(2)$—S—$M(1)$ decrease, whereas S—M, and S—S—M and S—M—S increase with the Cu content. Also, the mean bond lengths S—S and M—S are halfway along the first-row transition-element pyrites and the mean bond lengths S—M—S are the higher, as expected.

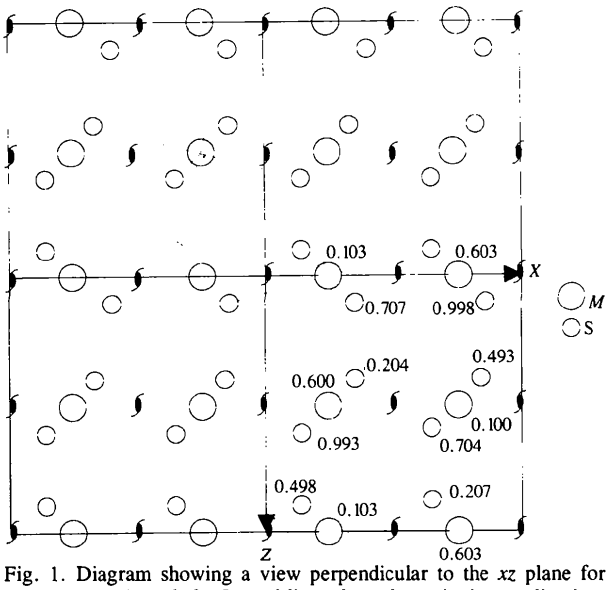

Fig. 1. Diagram showing a view perpendicular to the xz plane for structures (1) and (2). Dotted lines show the cationic coordination.

In spite of this noncubic symmetry in villamaninite, the unit-cell parameters are close to the cubic values; so, the unit cell of villamaninite is pseudocubic. The models explaining the bonding of the first-row transition-element pyrites (Bither, Bouchard, Cloud, Donohue & Siemons, 1968; Bröstigen & Kjekshus, 1970; Goodenough, 1972) attribute the increase in the metal–sulfur bond length to an increase in the number of antibonding electrons. Assuming this fact, a linear correlation between cell parameter and $N_{e_g^*}$ ($N_{e_g^*}$ being the formal number of electrons filling the e_g^* antibonding levels, $N = 0$ for FeS_2, $N = 1$ for CoS_2, $N = 2$ for NiS_2, $N = 3$ for CuS_2) is observed (Klemm, 1962; Bouchard, 1968; Shimazaki & Clark, 1970; Vaughan & Craig, 1978; Paniagua *et al.*, 1987). On this basis, the expected mean unit-cell parameter for any compound of the FeS_2–CoS_2–NiS_2–CuS_2 series can be calculated from the four end-term cell parameters. These calculated values are $a = 5.719$ Å for (1) ($N_{e_g^*} = 2.40$) and $a = 5.715$ Å for (2) ($N_{e_g^*} = 2.36$), showing a good agreement with the experimental values in Table 2.

4. Discussion in favor of monoclinic model

On the basis of the results obtained it is clear that villamaninite is not cubic and the best structure refinement is obtained in the monoclinic space group. This is also supported by two other aspects. First, the villamaninite from Spain is optically anisotropic, which by theory means it is noncubic. The second aspect is based on the results of previous studies on villamaninite (Paniagua, 1991; Friedl *et al.*, 1991), as is discussed below.

The presence of trace metals seems to be controlled by the substitution of Fe by Ni and Cu on the cation sites, which leads to an increase in the cell size. The substitution of S by Se plays a significant role in the stabilization of the pyrite structure for the Cu- and Ni-rich disulfides and facilitates the substitution of the major cations of the first long period by minor elements of the second and the third long periods. The presence of Cu and/or Ni facilitates the trace metal introduction, possibly because of its influence on the cell size as a result of filling the antibonding levels. Direct substitution between divalent cations and coupled substitution of two divalent cations by one trivalent cation plus a monovalent one are deduced (Paniagua *et al.*, 1987). These different types of cationic substitution can be related with the expected Jahn–Teller distortion of the octahedral coordination for Cu^{2+}. The dominancy of Cu^{2+} as a major cation and its Jahn–Teller distortion could explain the slight deviation from cubic symmetry, leading to monoclinic.

On the other hand, the ^{197}Au Mössbauer study of villamaninite suggests that the gold is present as a chemically bound impurity in the villamaninite structure, with two absorption peaks with different isomer

Table 4. *Atomic coordinates of the pyrite and coordinates of the villamaninite in the idealized $Pa\bar{3}$ pyrite structure, from the coordinates in the monoclinic model*

	Pyrite			(1)			(2)		
	x	*y*	*z*	*x* Δx*	*y* Δy*	*z* Δz*	*x* Δx*	*y* Δy*	*z* Δz*
M(1)	1/2	0.0	1/2	0.491 (1)	0.006	0.497 (1)	0.503 (1)	0.003	0.498 (1)
				0.009	−0.006	0.003	−0.003	−0.003	0.002
M(2)	0.0	1/2	1/2	0.999 (1)	0.502 (2)	0.504 (1)	0.002 (1)	0.498 (1)	0.501 (1)
				−0.001	−0.002	−0.004	−0.002	0.002	−0.001
S(1)	0.386	0.386	0.386	0.395 (1)	0.399 (3)	0.403 (2)	0.397 (1)	0.394 (1)	0.396 (1)
				−0.009	−0.013	−0.017	−0.011	−0.008	−0.011
S(2)	0.114	0.886	0.386	0.100 (2)	0.898 (3)	0.400 (2)	0.112 (1)	0.894 (2)	0.391 (1)
				0.014	−0.012	−0.014	0.002	−0.008	−0.005
S(3)	0.616	0.616	0.616	0.603 (1)	0.606 (2)	0.609 (1)	0.606 (1)	0.604 (1)	0.605 (1)
				0.013	0.010	0.007	0.010	0.012	0.011
S(4)	0.886	0.114	0.614	0.893 (1)	0.105 (3)	0.608 (1)	0.903 (1)	0.103 (1)	0.602 (1)
				−0.007	0.009	0.008	−0.017	0.011	0.012

* Difference between the coordinates of the pyrite and the idealized ones of the villamaninite.

Table 5. *Selected bond lengths (Å) and angles (°) for (1) and (2), with e.s.d.'s in parentheses*

	(1)	(2)
M(1)—S(1)	2.37 (1)	2.385 (9)
M(1)—S(2)	2.38 (1)	2.388 (9)
M(1)—S(3)	2.46 (1)	2.429 (8)
M(1)—S(4)	2.45 (1)	2.428 (8)
M(2)—S(1)	2.41 (1)	2.408 (8)
M(2)—S(2)	2.41 (1)	2.428 (9)
M(2)—S(3)	2.410 (8)	2.411 (7)
M(2)—S(4)	2.42 (1)	2.394 (8)
S(1)—S(3)	2.050 (4)	2.068 (2)
S(2)—S(4)	2.051 (4)	2.071 (3)
S(2)—*M*(1)—S(1)	88.6 (4)	86.9 (3)
S(3)—*M*(1)—S(1)	177.4 (6)	179.3 (3)
S(3)—*M*(1)—S(2)	93.7 (4)	92.8 (3)
S(4)—*M*(1)—S(1)	93.2 (4)	94.3 (3)
S(4)—*M*(1)—S(2)	177.9 (6)	178.4 (4)
S(4)—*M*(1)—S(3)	84.5 (3)	86.0 (2)
S(2)—*M*(2)—S(1)	86.7 (4)	85.5 (3)
S(3)—*M*(2)—S(1)	179.8 (2)	179.8 (1)
S(3)—*M*(2)—S(2)	93.2 (3)	94.3 (3)
S(4)—*M*(2)—S(1)	93.7 (4)	92.8 (3)
S(4)—*M*(2)—S(2)	179.5 (5)	178.1 (4)
S(4)—*M*(2)—S(3)	86.4 (3)	87.4 (2)
S(3)—S(1)—*M*(1)	106.2 (3)	104.8 (2)
S(3)—S(1)—*M*(2)	105.2 (4)	104.7 (2)
S(4)—S(2)—*M*(1)	104.9 (4)	103.9 (2)
S(4)—S(2)—*M*(2)	105.0 (3)	103.6 (2)
M(2)—S(1)—*M*(1)	113.1 (5)	114.0 (3)
M(2)—S(2)—*M*(1)	114.3 (5)	114.7 (3)
M(2)—S(3)—*M*(1)	114.1 (4)	113.5 (3)
M(2)—S(4)—*M*(1)	112.8 (4)	112.7 (3)

shifts and high quadrupole splittings, clearly different from that previously observed for gold impurities bound in pyrite. Gold replacing a transition metal in villamaninite should create an environment very similar to that of gold replacing iron in FeS_2, with a single absorption peak where the electric quadrupole splittings are very small (Marion, Wagner & Regnaurd, 1989). The presence of two absorption peaks can be related to two different cationic sites with different oxidation states for Au. An explanation for the comparatively large quadrupole splitting of gold in the villamaninite lattice *versus* the pyrite lattice could be the trend of gold having one or several Se neighbors replacing S. This might cause both substantial electric quadrupole interactions and small isomer shifts compared with gold in pyrite. Different numbers and arrangements of S and Se neighbors could also explain the asymmetry of the Mössbauer spectra, producing different values for the isomer shifts and electric quadrupole splitting. This hypothesis is also coherent with the monoclinic model for the villamaninite.

5. Conclusions

Considering the good results of the structural refinements of the villamaninite in space group $P12_11$ and the unsuccessful results in other subgroups of space group $Pa\bar{3}$ of the pyrite-type structure, it is clear that villamaninite is monoclinic. This fact agrees with the presence of Cu^{2+} as a major cation in villamaninite, because a distortion of the octahedral site resulting from the Jahn–Teller effect is expected.

Villamaninite is pseudocubic and a monoclinic model is also acceptable on the basis of the following points (i) the observed optical anisotropy; (ii) the relationships between major and trace elements in cationic substitution; (iii) the fact that Mössbauer spectroscopy experiments state different cation sites for Au, which is consistent with the $P12_11$ space group.

The villamaninite structure can be considered as intermediate between the cubic pyrite-type structure and the monoclinic derivative, related to the entry of Au in this type of structure, as it does in calaverite and low-temperature Au-bearing arsenopyrite.

Part of this work was supported by a Grant Research of the Spanish 'Ministerio de Educación y Ciencia' to one of the authors (AP) and a Spanish–German Integrate Action of Research.

References

Bayliss, P. (1977*a*). *Am. Mineral.* **62**, 369–373.
Bayliss, P. (1977*b*). *Am. Mineral.* **62**, 1168–1172.

Bayliss, P. (1977*c*). *Mineral. Mag.* **41**, 545.
Bayliss, P. (1989). *Am. Mineral.* **74**, 1168–1176.
Bayliss, P. & Stephenson, N. C. (1968). *Mineral. Mag.* **36**, 940–947.
Bither, T. A., Bouchard, R. J., Cloud, W. H., Donohue, P. C. & Siemons, W. J. (1968). *Inorg. Chem.* **7**, 2208–2220.
Bouchard, R. J. (1968). *Mat. Res. Bull.* **3**, 563–570.
Bröstigen, G. & Kjekshus, A. (1970). *Acta Chem. Scand.* **24**, 2993–3012.
Cabri, L. J., Harris, D. C., Stewart, J. M. & Roland, J. F. (1970). *Proc. Aust. Inst. Min. Metall.* **233**, 95–100.
Finklea III, S. L., Cathey, L. & Amma, E. L. (1976). *Acta Cryst.* A**32**, 529–537.
Friedl, J., Paniagua, A. & Wagner, F. E. (1991). *Neues Jahrb. Mineral. Abh.* **163(2/3)**, 247–256.
Gibbons, G. S. (1967). *Am. Mineral.* **52**, 359–370.
Giese, R. F. & Kerr, P. F. (1965). *Am. Mineral.* **50**, 1002–1014.
Goodenough, J. (1972). *J. Solid State Chem.* **5**, 144–152.
Grant, D. F. & Gabe, E. J. (1978). *J. Appl. Cryst.* **11**, 114–120.
Johan, Z., Marcoux, E. & Bonnemaison, M. (1989). *C. R. Acad. Sci. Paris II*, **308**, 185–191.
King, H. E. & Prewitt, Ch. T. (1979). *Am. Mineral.* **64**, 1265–1271.
Klemm, D. D. (1962). *Neues Jahrb. Mineral. Monatsh.* pp. 6–91.
Lehmann, M. S. & Larsen, F. K. (1974). *Acta Cryst.* A**30**, 580–584.
Marcoux, E., Bonnemaison, M., Braux, C. & Johan, Z. (1989). *C. R. Acad. Sci. Paris II*, **308**, 293–300.
Marion, P. H., Wagner, F. E. & Regnaurd, J. R. (1989). *Ind. Miner.* pp. 112–118.
Moreiras, D., Marcos, C., Díaz-Fernández, M. R. & García-Granda, S. (1991). *Neues Jahrb. Mineral. Abh.* **163(2/3)**, 254–256.
Motherwell, W. D. S. & Clegg, W. (1978). *PLUTO. Program for Plotting Molecular and Crystal Structures*. University of Cambridge, England.
Nardelli, M. (1983). *Comput. Chem.* **7**, 95–98.
Oudin, E., Marchig, V., Risch, H., Lalou, C. & Brichet, E. (1990). *C. R. Acad. Sci. Paris II*, **310**, 221–226.
Paniagua, A. (1989). *Neues Jahrb. Mineral. Abh.* **160**(1), 8–11.
Paniagua, A. (1991). *Neues Jahrb. Mineral. Abh.* **163**(2/3), 241–247.
Paniagua, C. A., Marcos, P. C., Moreiras, B. D. & Gonzáles, P. J. (1987). *Bol. Soc. Esp. Mineral.* **10**(2), 177–185.
Pertlik, F. (1984). *Z. Kristallogr.* **169**, 227–236.
Ramdohr, P. (1980). *The Ore Minerals and Their Intergrowths*. Oxford: Pergamon Press.
Robinson, K., Gibbs, G. V. & Ribbe, P. H. (1971). *Science*, **172**, 567–570.
Schoeller, W. R. & Powell, A. R. (1920). *Mineral. Mag.* **19**, 14–18.
Sheldrick, G. M. (1976). *SHELX*76. *Program for Crystal Structure Determination*. University of Cambridge, England.
Sheldrick, G. M. (1985). *SHELXS*86. *Crystallographic Computing* 3, edited by G. M. Sheldrick, G. Kruger & R. Goddard, pp. 175–189. Oxford: Clarendon Press.
Shimazaki, H. & Clark, L. A. (1970). *Can. Mineral.* **10**, 648–664.
Stanton, R. L. (1975). *Can. Mineral.* **6**, 87–118.
Taylor, L. A. & Kullerud, G. (1972). *Neues. Jahrb. Mineral. Monatsh.* **10**, 458–464.
Vaughan, D. J. & Craig, J. R. (1978). *Mineral Chemistry of Metal Sulfides*. Cambridge University Press.
Wyckoff, R. W. G. (1963). *Crystal Structures*, 2nd ed., Vols. 1–6. New York: Interscience. Encyclopedic compilation.
Ypma, P. J. M., Evers, H. J. & Woensdregt, G. F. (1968). *Neues Jahrb. Mineral. Monatsh.* pp. 174–192.